

# Supplementary Material — “Ice thickness distribution of all Swiss glaciers based on extended ground penetrating radar data and glaciological modeling”

Melchior Grab, Enrico Mattea, Andreas Bauder, Matthias Huss, Lasse Rabenstein, Elias Hodel, Andreas Linsbauer, Lisbeth Langhammer, Lino Schmid, Gregory Church, Sebastian Hellmann, Kevin Délèze, Philipp Schaer, Patrick Lathion, Daniel Farinotti, Hansruedi Maurer

## Overview

This document provides illustrations and tables as supplementary material to the publication "Ice thickness distribution of all Swiss glaciers based on extended ground penetrating radar data and glaciological modeling". All material is based on data which are available in the SwissGlacierThickness-R2020 data package (Grab et al., 2020), except some ice thickness data measured with GPR which were already published by various researchers on GlaThiDa 3.0.1. (GlaThiDa Consortium, 2019), and ice thickness data from two GPR campaigns (Sharp et al., 1993; Huybrechts et al., 2008).

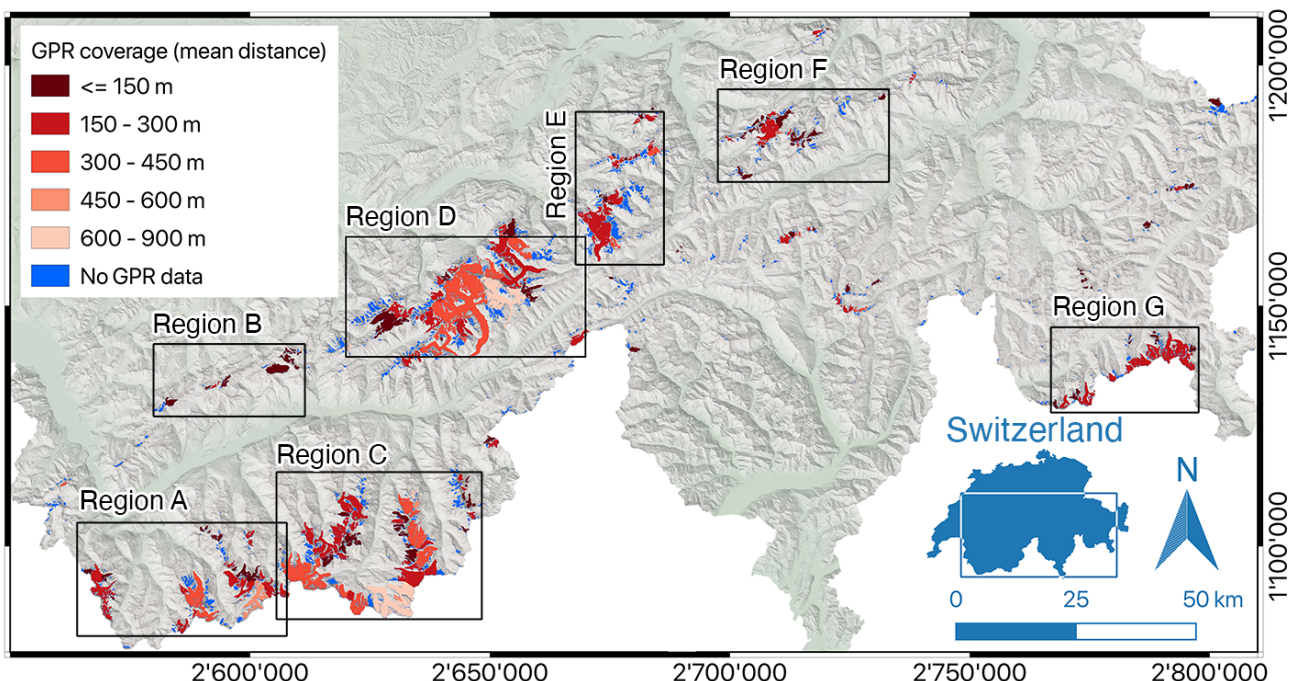


Figure S1: Reproduced after Fig. 1a of the main manuscript: Glacier outlines of the SGI 2016 (after GLAMOS, 2020b) coloured in blue for glaciers for which no GPR data exists and in red for glaciers with GPR data. Closeups to regions A to G are provided below in Figures S2-S8. Background: Hillshade from swissALTI3D after Swisstopo (2019)

# 1 Glaciers with- and without GPR data

Here, a more complete version of table 2 presented in the main study is given. For computing the interpolated ice thickness distributions and glacier bed topography maps, all available GPR data has been used (Table S1), except the data recorded in spring 2020. For the spring 2020 data, see data sets cited by [9] in Table S1 and the data sets for which a profile length is given in Table S2.

Table S1: List of glaciers for which GPR data were used for ice thickness modelling. The following information is provided: areas according to the SGI2016 ( $A$ ), volumes ( $V_{2016}$ ), mean thickness ( $h_{\text{mean}}$ ) and maximum thickness ( $h_{\text{max}}$ ) of the interpolated ice thickness distributions, mean distance to closest GPR point ( $d_{\text{mean-gpr}}$ ), total profile lengths (p. length), year of the GPR survey, and the corresponding references of the GPR data. For discussion of this table see main study

SGI-id	Glacier Name	$A$ (km $^2$ )	$V_{2016}$ (km $^3$ )	Interpolation $h_{\text{mean}}(m)$ $h_{\text{max}}(m)$	$d_{\text{mean-gpr}}$ (m)	p. length (km)	GPR survey year(s)	GPR survey references <sup>1</sup>
B36/26	Grosser Aletsch	78.5	11.70	147	794	327	118.6	1958,2009,2011 [3,16,27]
B56/07	Gorner	41.2	3.71	91	385	810	34.4	1990-2012 [12,14,16,17]
B40/07	Fiescher	29.8	3.52	117	437	648	17.8	2011 [16,26]
A54g/11	Unteraar	22.7	2.85	126	377	285	29.7	1086-2002,2012 [1,19,21,22]
B43/03	Rhone	14.6	1.46	99	419	181	30.2	2003,2008 [4,19]
A51d/10	Huefi	12.6	1.23	104	305	160	18.4	2018 [8]
B83/03	Corbassiere	14.9	1.22	82	247	425	31.4	1988,1998,2011 [7,16]
B36/01	Oberaletsch	17.1	1.20	68	225	350	74.4	2009,2011,2017,2019 [8,27,31,32]
B57/05	Zmutt	14.8	1.02	70	265	332	20.8	2012,2017 [8,16]
A55b/13	Alpetli	12.0	1.02	91	228	146	46.5	2012,2019 [8,16]
B56/03	Findelen	13.9	1.01	74	206	254	29.5	2008,2012,2017 [8,12,16]
E22/03	Morteratsch	14.9	0.90	61	281	225	25.5	2001,2002,2017 [8,13]
A54e/24	Trift	14.6	0.80	55	324	226	32.6	2002,2008,2012 [16,19]
B82/27	Otemma	12.6	0.78	62	256	533	19.7	2011,2016 [8,16]
B63/05	Zinal	13.5	0.78	58	208	266	17.5	2007,2010,2016,2017 [8,11,25]
B60/09	Turtmann	10.7	0.66	61	210	217	18.1	2012 [16]
A55f/03	Raetzli	7.3	0.64	87	208	57	47.3	2016,2017 [8]
A54l/19	Untergrindelwald	9.2	0.60	68	197	430	9.1	2019 [8]
B52/29	Allalin	9.1	0.58	64	242	327	32.1	1982,2008,2013,2017 [16,20]
A54i/05	Gauli	10.8	0.57	53	253	405	36.5	2012 [16,19]
B53/04	Fee	13.8	0.57	41	161	346	10.8	2013,2017 [8,16,28]
B54/03	Ried	7.2	0.55	76	195	308	4.1	2013 [28]
B56/28	u. Theodul	9.6	0.55	58	184	391	8.7	2013 [29]
B72/15	Montmine	10.1	0.54	54	155	416	5.4	2012 [16]
C83/12	Forno	6.0	0.52	88	300	164	9.9	2017 [8]
B72/11	Ferpecle	9.1	0.50	56	148	325	5.5	2012 [16]
B31/04	Lang	8.0	0.49	59	204	185	17.9	2012,2019 [8,16]
A54l/31	o. Ischmeer E	7.3	0.48	68	273	331	4.1	2019 [8]
B85/16	Saleina	6.7	0.46	68	203	175	3.8+6.7	2013,2020 [8,9,16]
B90/02	Trient	5.8	0.41	71	188	175	2.2+7.6	2013,2020 [8,9,16]
B82/14	Gietro	5.1	0.38	75	224	162	10.5	1997,2011,2018 [7,8,16]
B82/19	Breney	7.1	0.38	53	212	237	12.6	2011,2016 [8,16]
A54j/02	Rosenlau	5.4	0.34	63	220	125	8.4	2019 [8]
A54l/04	Obgrindelwald	8.3	0.34	44	180	256	6.2	2010,2019 [8,19]
B73/14	Arolla	5.1	0.30	60	193	229	20.2	2011,2016 [8,16]
A50i/19	Clariden	4.7	0.30	68	216	118	9.5	1992,2018 [8,19]
E23/06	Tschierva	5.6	0.27	49	157	218	9.7	2017 [8]
B82/36	Montdurand	6.2	0.27	43	154	319	9.1	2011 [16]
B45/04	gries	4.6	0.26	55	209	192	6.8	1999 [5]
B64/02	Moiry	5.0	0.26	51	178	199	17.2	2012 [16]
A54m/21	Tschingel	5.1	0.25	56	137	190	9.7	2019 [8]
B62/10	Moming	5.4	0.24	45	189	282	8.1	2017 [8]
B30/06	Tellin	5.1	0.23	50	139	94	35.1	2012,2019 [8,16]
B52/24	Schwarzberg	5.1	0.23	44	124	162	12.0	2008 [16]
A54m/12	Rottal	3.6	0.23	68	214	276	3.1	2019 [8]
E23/11	Roseg	6.6	0.22	35	97	168	9.7	2017 [8]
B36/21	Mittelaletsch	6.6	0.22	32	143	282	8.0	2009,2017 [8,27]
B74/08	Cheillon	3.5	0.21	60	194	104	10.7	2016,2018 [8]
B22/01	Tsanfleuron	2.4	0.21	84	175	87	14.7	2010,2012 [6,18]
B73/16	Tsidjiore	2.8	0.20	69	180	128	19.8	2011,2016,2018 [8,16]
B55/04	Hohberg	3.0	0.19	65	164	100	9.4	2017 [8]
B58/02	Hohlicht	4.5	0.19	42	194	134	9.0	2017 [8]
A54e/12	Stein	5.6	0.19	34	103	198	10.4+5.7	2013,2020 [8,9,16]
B58/08	Bis	4.2	0.19	44	153	187	12.3	2012,2017 [8,16]
B55/18	Mellich	3.1	0.17	56	113	139	9.3	2017 [8]
B73/12	Arollahaut	3.6	0.16	46	137	205	7.2	1991,2016 [8,19]

Continued on Next Page...

Table S1: List of glaciers with GPR data (continued)

SGI-id	Glacier Name	$A$ (km $^2$ )	$V_{2016}$ (km $^3$ 5)	Interpolation $h_{\text{mean}}(m)$	$h_{\text{max}}(m)$	$d_{\text{mean-gpr}}$ (m)	p. length (km)	GPR survey year(s)	GPR survey references <sup>1</sup>
B57/16	Trift (Zermatt)	2.1	0.14	68	212	125	3.8	2017	[8]
C93/04	Palue	5.4	0.14	29	84	155	10.6	2017	[8]
A10g/05	Silvretta	2.7	0.14	55	120	142	4.5	2007	[4]
A54g/03	Oberaar	4.0	0.14	40	127	113	22.8	2012	[16,19]
C84/16	Albigna	2.4	0.14	58	152	179	4.9	2017	[8]
A51d/15	Brunni	2.2	0.12	53	152	127	4.4	2018	[8]
A54m/19	Breithorn	2.5	0.12	52	189	159	3.8	2019	[8]
B52/32	Hohlaub	2.2	0.11	51	127	254	1.9	2013	[16]
B57/10	Hohwaeng	2.2	0.11	49	119	106	4.2	2017	[8]
A50i/12	Biferten	2.6	0.11	47	110	96	7.0	2018	[8]
B56/31	Furgg	3.8	0.10	28	92	382	6.2	2013	[29]
B56/14	Adler	2.1	0.096	46	133	183	4.7	2017	[8]
B85/23	Orny	1.3	0.093	71	134	98	4.4+2.2	2013,2020	[8,9,16]
B34/02	Baltschieder	3.6	0.088	23	81	213	7.6	2013	[16]
B57/14	Gabelhorn	1.8	0.083	46	198	198	2.7	2017	[8]
C01/04	Weissmies	1.9	0.082	41	117	92	5.7	2018	[8]
B55/07	Festi	1.8	0.080	44	122	165	4.1	2017	[8]
A55c/13	Laemmern	2.3	0.079	34	86	137	6.4	2017	[8]
A54j/03	Hengstener NE	1.7	0.077	47	117	272	2.1	2019	[8]
E50/07	Tiatscha	1.9	0.076	43	92	885	4.5	2007	[4]
A51c/02	Griess	2.1	0.076	41	104	120	5.6	2018	[8]
B56/30	Theodul	2.4	0.075	32	105	151	6.3	2013	[25]
B34/03	i. Baltschieder	1.7	0.075	43	109	259	2.0	2013	[29]
B41/07	Minstiger	2.2	0.074	32	96	147	4.3	2013	[16]
E26/01	Fedoz	1.9	0.074	40	112	228	3.3	2017	[8]
B55/36	Mellich	1.5	0.072	47	125	130	5.9	2017	[8]
C05/02	Alpjer	2.1	0.071	32	84	155	4.2	2018	[8]
B53/08	Bider	1.3	0.068	54	112	465	0.2	2013	[28]
A54e/06	Wenden	1.7	0.068	41	146	186	2.8	2013	[16]
A54m/06	Giesen	1.7	0.063	43	120	254	1.2	2019	[8]
B55/08	Kin	1.2	0.062	53	144	112	3.7	2017	[8]
A14g/02	Medel z	1.8	0.062	35	74	154	2.5	2018	[8]
B85/07	Neuve	1.9	0.062	32	117	205	1.0+1.9	2013,2020	[8,9,16]
E25/04	Tremoggia	1.8	0.061	35	85	177	4.1	2017	[8]
B56/10	Monte Rosa	1.3	0.060	46	97	468	17.4	2008	[16]
A50i/06	Limmern	2.0	0.060	37	81	142	3.7	2018	[8]
B47/04	Kaltwasser	1.6	0.060	37	94	138	3.2	2018	[8]
A54m/05	Guggi	1.6	0.059	43	97	138	2.4	2019	[8]
A50k/04	Glaernisch	1.4	0.058	46	132	156	3.3	2018	[8]
A14g/16	Medel E	1.2	0.056	49	118	125	1.9	2018	[8]
B62/07	Weisshorn	1.7	0.054	32	87	134	3.9	2017	[8]
A54m/03	Eiger	1.5	0.052	36	93	176	2.0	2019	[8]
B73/15	Piece	1.3	0.051	40	133	178	3.7	2016	[8]
B55/12	Weingarten	1.3	0.051	39	103	91	4.6	2017	[8]
A13n/06	Paradies	1.9	0.049	29	107	165	3.0	2018	[8]
B62/08	Weisshorn S	1.3	0.048	38	121	246	1.1	2017	[8]
B73/26	Vouasson Z	1.5	0.048	32	94	177	2.0	2018	[8]
C02/04	Rossboden	1.2	0.048	39	116	256	1.1	2018	[8]
B58/04	Schali W	1.7	0.048	28	67	190	4.8	2017	[8]
A14g/17	Medel W	1.1	0.047	44	99	168	1.1	2018	[8]
B57/11	Arben W	1.1	0.045	42	115	109	1.7	2017	[8]
B85/04	Dolent	1.2	0.044	38	68	236	0.4+0.7	2013,2020	[8,9,16]
B53/11	Balfrin	1.7	0.044	24	87	610	0.6	2013	[28]
A12e/04	Porchabella	1.4	0.043	31	66	109	3.8	2017	[8]
B53/07	Hohbalm	1.7	0.041	25	66	323	1.1	2013	[28]
B55/09	King SW	0.9	0.038	42	122	84	3.0	2017	[8]
C00/08	Zwischbergen	1.3	0.038	30	71	224	1.6	2018	[8]
E23/03	Misaun	0.8	0.037	45	89	62	4.0	2017	[8]
C84/20	Castel N	1.3	0.037	31	77	109	3.5	2017	[8]
B31/02	Jaegi	1.3	0.036	26	66	191	1.5	2019	[8]
B73/24	Aig. Rouges Z	0.8	0.036	46	108	185	0.8	2018	[8]
B74/18	Prafleur	0.8	0.036	42	84	106	2.0	2018	[8]
A51e/37	Tiefen	2.2	0.034	16	54	304	5.9	2012	[15]
B72/06	Moiry S	0.5	0.033	72	154	231	15.8	2012	[16]
B75/06	Granddesert	1.1	0.033	30	69	127	2.2	2018	[8]
A56d/01	Dungel	0.6	0.032	56	112	82	2.6	2017	[8]
C84/09	Cantun	0.8	0.032	44	134	69	2.9	2017	[8]
A50j/06	Im Griess	1.2	0.032	33	71	160	4.0	2018	[8]
C93/09	Cambreña	1.3	0.032	26	56	102	3.7	2017	[8,30]
A14d/10	Gufer N	1.1	0.032	29	63	102	3.2	2018	[8]

Continued on Next Page...

Table S1: List of glaciers with GPR data (continued)

SGI-id	Glacier Name	$A$ (km $^2$ )	$V_{2016}$ (km $^3$ 5)	Interpolation $h_{\text{mean}}(m)$	$h_{\text{max}}(m)$	$d_{\text{mean-gpr}}$ (m)	p. length (km)	GPR survey year(s)	GPR survey references <sup>1</sup>
B74/11	Darrey	1.3	0.030	23	73	271	1.4	2018	[8]
B85/08	Neuve N	1.3	0.030	23	59	261	0.1+1.4	2013,2020	[8,9,16]
B21/05	Diablerets	0.7	0.029	39	68	1240	11.7	2010	[18]
B36/18	Zenbachen	0.8	0.029	33	72	361	0.7	2017	[8]
A14p/01	Vorab	1.2	0.028	26	63	109	3.2	2018	[8]
B23/03	Wildhorn NE	0.8	0.028	34	86	92	3.5	2017	[8]
B55/19	Langflue Z	0.9	0.027	30	72	185	1.8	2017	[8]
E45/08	Grialetsch	1.2	0.026	24	59	250	2.4	2017	[8]
B55/16	Alphubel	0.8	0.026	31	81	120	1.9	2017	[8]
B57/19	Rothorn Zerm.	0.8	0.026	32	69	105	2.1	2017	[8]
A54e/13	Steinlimmi	1.5	0.025	17	53	144	10.4+1.1	2013,2020	[8,9,16]
C85/06	Bondasca	1.0	0.025	26	60	82	3.6	2017	[8]
A14m/09	Punteglias	0.7	0.025	42	136	58	3.1	2018	[8]
E44/04	Sarsura	0.9	0.025	34	68	97	2.9	2017	[8]
B52/06	Rotblatt S	0.7	0.024	34	93	87	1.9	2018	[8]
B43/12	Tiertaelli	1.0	0.024	25	74	155	9.5	2008	[4]
A55f/01	Ammerten	0.9	0.024	27	71	116	2.8	2017	[8]
A51h/15	Titlis	0.6	0.024	38	69	350	0.5	1994	[19]
A51d/04	Stafel	0.7	0.023	41	98	156	1.4	2018	[8]
A54i/10	Renfen	0.8	0.022	27	110	1158	0.7	2019	[8]
A14n/05	Frisal W	0.5	0.022	48	127	86	1.7	2018	[8]
E23/04	Tschierva	0.6	0.021	39	84	87	1.7	2017	[8]
A51d/07	Bocktschingel	0.8	0.019	31	80	78	2.6	2018	[8]
A51d/06	Ruchen	0.8	0.019	29	73	70	3.0	2018	[8]
B93/06	Plan Neve NE	0.6	0.019	32	71	305	0.5	2013	[6]
C01/07	Laggin	0.7	0.018	25	59	129	1.3	2018	[8]
B74/09	Luette	0.6	0.018	30	66	108	1.4	2018	[8]
C14/10	Basodino	1.6	0.018	14	25	114	4.3	2006	[19]
A55c/11	Lammeren	0.57	0.018	31	83	69	2.7	2017	[8]
E45/11	Grialetsch E	0.83	0.018	26	62	102	2.4	2017	[8]
A55c/14	Steghorn	0.35	0.017	50	114	56	1.8	2017	[8]
C01/09	Holutrift	0.55	0.017	29	67	174	1.0	2018	[8]
A14f/15	Lavaz	0.64	0.017	26	87	342	0.4	2018	[8]
B62/13	Turtmann	0.26	0.017	63	122	164	11.1	2012	[16]
E35/17	Calderas	0.61	0.017	28	74	71	2.5	2017	[8]
A14f/12	Valdraus	0.45	0.016	37	80	168	0.9	2018	[8]
A55f/08	Chilchli	0.37	0.016	43	83	61	3.6	2017	[8]
B30/28	Tellin SW	0.56	0.016	27	70	96	8.2	2012,2019	[8,16]
B75/12	Montfort	0.58	0.016	27	58	21	5.2	2013,2018	[6,8]
A14c/03	Fanell	0.87	0.016	19	51	125	2.5	2018	[8]
A56d/04	Gelten NE	0.72	0.015	21	43	267	1.9	2017	[8]
A56d/05	Gelten SW	0.51	0.015	29	67	121	1.3	2017	[8]
B55/37	Langflue	0.46	0.015	33	71	48	3.3	2017	[8]
C02/02	Bodmer	0.52	0.015	27	71	100	1.1	2018	[8]
A13n/04	Zapport	1.30	0.014	12	30	320	0.5	2018	[8]
B75/09	Mont Fort	0.35	0.014	39	102	100	0.5	2018	[8]
A14l/22	Gliems	0.47	0.013	34	65	78	1.8	2018	[8]
A14l/11	Cavrein	0.38	0.012	37	83	92	1.2	2018	[8]
A50i/13	Todi N	0.41	0.011	33	60	74	1.4	2018	[8]
A50i/18	Sand W	0.43	0.011	31	63	353	0.3	2018	[8]
A50j/07	Iswandli	0.35	0.011	37	92	125	1.0	2018	[8]
A51h/34	Stotzig Egg	0.30	0.011	36	84	145	0.8	1994	[19]
B44/03	Mutt	0.36	0.011	27	54	71	1.5	2009	[6]
A51d/18	Stalden	0.48	0.011	22	44	97	0.9	2018	[8]
B30/27	Tennbach	0.30	0.010	33	59	87	3.3	2012,2019	[8,16]
A50i/17	Sand E	0.43	0.010	29	46	201	0.6	2018	[8]
A14d/17	Lenta	0.77	0.010	17	36	275	1.2	2018	[8]
A51f/16	Stei	0.36	0.0098	28	59	82	8.6+1.3	2013,2020	[8,9,16]
E22/11	Fortezza	0.45	0.0096	23	42	181	0.6	2017	[8]
B31/16	Jegi W	0.34	0.0095	27	51	198	0.2	2019	[8]
C01/03	Talli W ZwBerg	0.38	0.0094	26	59	122	0.8	2018	[8]
A14p/03	Segnes	0.51	0.0090	20	57	297	1.2	2011	[6]
B73/34	Tsijiore Nouve	0.27	0.0087	32	80	145	0.2	2016	[8]
B75/07	Petit Mont Fort	0.26	0.0086	33	56	128	0.5	2018	[8]
A55d/05	Strubel	0.38	0.0086	23	46	71	1.5	2017	[8]
B16/01	Sexrouge	0.26	0.0081	31	57	28	3.1	2012	[6]
C44/02	Bresciana	0.42	0.0081	22	41	233	0.7	2018	[8]
B58/26	Hohlicht	0.26	0.0081	31	53	187	0.3	2017	[8]
A55b/30	Kander SW	0.32	0.0080	29	50	109	0.9	2019	[8]
E42/10	Vallorgia	0.25	0.0078	32	72	88	1.0	2017	[8]

Continued on Next Page...

Table S1: List of glaciers with GPR data (continued)

SGI-id	Glacier Name	$A$ (km $^2$ )	$V_{2016}$ (km $^3$ 5)	Interpolation $h_{\text{mean}}(m)$	$h_{\text{max}}(m)$	$d_{\text{mean-gpr}}$ (m)	p. length (km)	GPR survey year(s)	GPR survey references <sup>1</sup>
E35/19	Err S	0.29	0.0075	27	58	82	0.9	2017	[8]
E35/15	Agnel	0.28	0.0074	27	66	85	1.1	2017	[8]
A14f/11	Sut	0.32	0.0073	23	43	76	1.1	2018	[8]
E23/02	Misaun S	0.25	0.0072	30	58	57	1.2	2017	[8]
C01/10	Sibiluflue	0.23	0.0068	29	63	115	0.4	2018	[8]
B32/05	Stampbach	0.20	0.0068	33	86	216	7.6	2013	[16]
A14m/05	Urlaun S	0.33	0.0066	24	48	174	0.7	2018	[8]
B36/11	Distel	0.33	0.0064	18	42	117	0.4	2017	[8]
E23/16	Murtel	0.30	0.0063	22	42	83	0.7	2013	[6]
B23/07	Wildhorn SW	0.26	0.0061	23	48	47	2.0	2017	[8]
E35/13	Trauntr Ovas W	0.20	0.0060	31	67	66	0.9	2017	[8]
A55f/07	Ammerte	0.33	0.0058	18	56	117	2.1	2017	[8]
B52/26	Fluchthorn W	0.27	0.0057	22	41	348	29.5	2008,2013	[16]
A51d/08	Halsifirn	0.29	0.0056	24	86	89	0.4	2018	[8]
A55b/16	Loetsche	0.73	0.0053	12	27	709	0.1	2018	[18]
A15b/04	Sardona	0.43	0.0052	15	29	268	0.5	2011	[6]
E23/18	Corvatsch	0.22	0.0046	22	48	90	1.2	2013	[6]
A12i/03	Err N	0.20	0.0044	23	49	88	1.3	2017	[8]
E42/08	Scalettawest	0.19	0.0041	23	42	100	0.7	2017	[8]
A51e/12	Sanktanna	0.20	0.0039	19	39	61	0.8	2013	[6]
A50j/13	Gruppen NE	0.16	0.0032	24	46	123	0.3	2018	[8]
A50i/25	Glarner Todi E	0.17	0.0030	23	53	55	0.8	2018	[8]
E33/01	Guglia	0.09	0.0030	33	59	62	0.3	2017	[8]
A51e/10	Gurschen	0.14	0.0029	21	37	46	0.8	2013	[6]
B47/05	Homattu N	0.16	0.0027	15	34	62	0.6	2018	[8]
A12e/10	Porchabella nw	0.07	0.0024	34	63	50	0.7	2017	[8]
E42/13	Porchabella ne	0.08	0.0023	29	55	93	0.7	2017	[8]
A12i/04	Piz d'Err N	0.10	0.0022	23	42	48	0.6	2017	[8]
B73/37	Vouasson S	0.05	0.0017	31	73	137	0.6	2018	[8]
B73/01	Tsarmine	0.09	0.0014	16	26	38	0.9	2015	[2]
A54m/02	Eigerwest	0.08	0.0013	19	41	69	0.6	1993	[19]
B45/35	Blinnenhorn	0.08	0.0013	13	71	173	6.8	1999	[5]
A50d/01	Pizol	0.07	0.0011	17	37	6	4.1	2010	[10]
C84/17	Bondasca	0.05	0.0008	17	36	121	0.8	2017	[8]
A55d/08	Grosstrubel NE	0.06	0.0008	13	24	85	0.3	2017	[8]
A51e/08	Schwarzbach	0.05	0.0005	10	15	133	0.1	2013	[6]
A55c/25	Grosstrubel SW	0.03	0.0003	11	20	73	0.3	2017	[8]
A12j/02	Err NW	0.02	0.0003	18	35	28	0.8	2017	[8]
A22/02	Blauschnee	0.03	0.0002	12	19	15	0.9	2011	[6]

<sup>1</sup>**GPR survey references:** [1] Bauder et al. (2003)<sup>b</sup>; [2] Capt et al. (2016)<sup>a</sup>; [3] Farinotti et al. (2009) after Thyssen and Ahmad (1969); [4] Farinotti et al. (2009)<sup>a</sup>; [5] Feiger et al. (2018)<sup>a</sup>; [6] Fischer et al. (2013)<sup>a</sup>, Huss and Fischer (2016)<sup>a</sup>; [7] VAW (1998)<sup>b</sup>; [8] Grab et al. (2020); [9] Grab et al. (2020) acquired in 2020; [10] Huss (2010)<sup>a</sup>; [11] Huss et al. (2008)<sup>a</sup>; [12] unpublished GPR data from 2008 (ETHZ) and 2012 (UZH, UFR)<sup>a</sup>; [13] Huybrechts et al. (2008); [14] Lüthi (2000)<sup>b</sup>; [15] Moll (2012)<sup>a</sup>; [16] Rutishauser et al. (2016)<sup>a</sup>; [17] Sugiyama et al. (2008)<sup>a</sup>; [18] unpublished GPR data from UFR<sup>a</sup>; [19] unpublished GPR data ETHZ<sup>b</sup>; [20] Waechter and Roethlisberger (1982)<sup>b</sup>; [21] Roethlisberger and Funk (1987)<sup>b</sup>; [22] Gudmundsson (1994) and Funk et al. (1994)<sup>b</sup>; [23] Lüthi (1994)<sup>b</sup>; [24] Sharp et al. (1993); [25] VAW (2010)<sup>b</sup>; [26] VAW (2011)<sup>b</sup>; [27] VAW (2012)<sup>b</sup>; [28] VAW (2014a)<sup>b</sup>; [29] VAW (2014b)<sup>b</sup>; [30] VAW (2017a); [31] VAW (2017b); [32] VAW (2019)

<sup>a</sup>retrieved from GlaThiDa Consortium (2019), <sup>b</sup>retrieved from GLAMOS (2020a)

Table S2: List of glaciers (with  $V_{2016} \geq 0.02 \text{ km}^3$ ) for which no GPR data were used for ice thickness modelling. The following information is provided: Areas according to the SGI2016 ( $A$ ), glacier volumes ( $V_{2016}$ ), mean thickness ( $h_{\text{mean}}$ ) and maximum thickness ( $h_{\text{max}}$ ) of the interpolated ice thickness distributions. For glaciers for which we acquired GPR data in spring 2020, mean distance to closest GPR point ( $d_{\text{mean-gpr}}$ ) and the total profile lengths are listed.

SGI-id	Glacier Name	$A$ ( $\text{km}^2$ )	$V_{2016}$ ( $\text{km}^3$ )	Interpolation	$d_{\text{mean-gpr}}$	profile length (km)
				$h_{\text{mean}}(m)$	$h_{\text{max}}(m)$	
A51g/05	Glatt (Erstfeld)	2.8	0.129	46	96	344
A51f/10	Damma	3.8	0.124	33	64	-
B40/06	Trift W (Fiescher)	1.9	0.091	45	102	-
B84/15	Valsorey	2.0	0.088	43	88	160
B82/41	Tsesette	2.1	0.081	39	75	-
B56/26	Breithorn (Zermatt)	2.0	0.069	36	64	-
A55b/02	Bluemlisalp (BE)	2.2	0.067	36	81	-
A51g/11	Bluemlisalp (UR)	2.2	0.066	36	68	174
A51f/23	Flachenstein	2.3	0.064	28	55	-
B36/17	Driest	1.8	0.062	32	63	-
A51f/15	Chelen	1.8	0.059	34	90	190
B84/17	Tseudeut	1.5	0.058	38	77	230
B84/04	Boveire	1.7	0.058	35	64	210
B51/13	Trift SE (Saas Grund)	1.6	0.055	35	91	-
B83/15	Follats	1.2	0.048	39	82	-
A54i/03	Grienbargli	1.3	0.046	35	58	-
A51g/18	Schlossberg (Erstfeld)	1.4	0.045	33	68	220
A51f/34	Ruti	1.5	0.045	30	54	-
B57/02	Matterhorn	1.6	0.043	27	49	-
A14n/08	Gaviolas	1.3	0.042	40	78	-
A54i/02	Hiendertellti	1.3	0.042	32	65	-
B72/07	Bricola	1.1	0.041	36	63	-
A51f/24	Wallenbur	1.4	0.041	29	55	-
B52/22	Seewjinen	1.4	0.040	30	69	-
A55b/18	Balmhorn	1.3	0.040	31	63	-
B90/04	Grands	1.5	0.039	26	45	121
B58/12	Abberg	1.1	0.038	35	68	-
A54l/38	Chall	0.8	0.036	45	90	-
A54g/25	Baechli	1.1	0.034	31	67	-
A55c/05	Schwarz	1.1	0.034	30	70	-
B72/08	Dent Blanche	1.1	0.034	31	57	-
B72/10	Manzettes	1.0	0.034	35	85	-
B51/05	Gruebu	1.0	0.034	32	62	-
B58/15	Ustelli	0.8	0.032	38	71	-
A54h/04	Grueben	1.1	0.030	28	62	-
A51e/35	Sidelen	1.0	0.030	30	55	-
B40/09	Finsteraahorn S	1.1	0.028	25	44	-
B33/02	Joli	0.9	0.028	31	59	-
A51f/13	Rotfirn	0.9	0.028	30	53	-
B84/11	Sonadon	0.9	0.027	29	76	169
B82/30	Epicoune	0.9	0.026	29	64	-
A54m/15	Schmadri	1.0	0.026	32	76	-
B41/05	Baechi	1.0	0.026	24	55	-
A51f/69	Maasplangg	0.8	0.026	31	50	199
B51/09	Fletschhorn	0.6	0.024	39	99	-
A51f/11	Sonadon	0.9	0.024	27	47	-
A10g/08	Verstankla	0.8	0.023	33	68	-
A51h/02	Griessen	0.9	0.023	32	69	177
A51f/32	Kartigel	1.0	0.023	23	55	-
B95/09	Mont Ruan E	0.7	0.023	30	61	-
B72/09	Dent Blanche SW	0.7	0.022	33	57	-
A54l/14	Schreck	0.8	0.022	31	50	-
B44/17	Geren	0.7	0.022	31	55	-
A51e/20	Witenwasseren	0.7	0.022	34	66	-
A51e/23	Mutten	0.8	0.021	30	55	-

Continued on Next Page...

Table S2: List of glaciers without GPR data (continued)

SGI-id	Glacier Name	$A$ (km $^2$ )	$V_{2016}$ (km $^3$ )	Interpolation	$d_{\text{mean-gpr}}$ (m)	profile length (km)
				$h_{\text{mean}}(m)$	$h_{\text{max}}(m)$	
B74/15	Ecoulaies	0.8	0.021	28	55	-
A51f/19	Brunnen W	0.7	0.020	28	46	-
A54f/07	Alpli	0.9	0.020	23	49	-
Smaller glaciers for which GPR data were recorded in 2020:						
A51g/12	Schloss (Isenthal)	0.73	0.0175	30	53	141
A51h/13	Firnalpeli	0.68	0.0171	25	54	169
B85/13	Planreuses	0.58	0.0169	29	46	252
B85/11	Treutsebo	0.38	0.0107	28	56	140
B85/20	Ravines Rousses	0.34	0.0102	30	62	94
A51h/11	Grassen	0.41	0.0085	21	39	216
A51h/22	Spannort SW	0.32	0.0079	25	42	96
A51h/23	F+B74irnalpeli E	0.30	0.0058	19	32	133
A51h/10	Grassen E	0.27	0.0056	21	36	278
A51g/10	Chessel	0.27	0.0049	23	41	84
A51h/08	Spannort SW	0.20	0.0040	21	31	153
A51f/86	Glatt	0.07	0.0017	25	44	101
A51h/26	Schloss	0.05	0.0011	23	41	140
1094 further glaciers		122.6	2.48	17	125	0
						0.0

## 2 Maps: GPR-coverage, ice thickness distribution, glacier bed topography

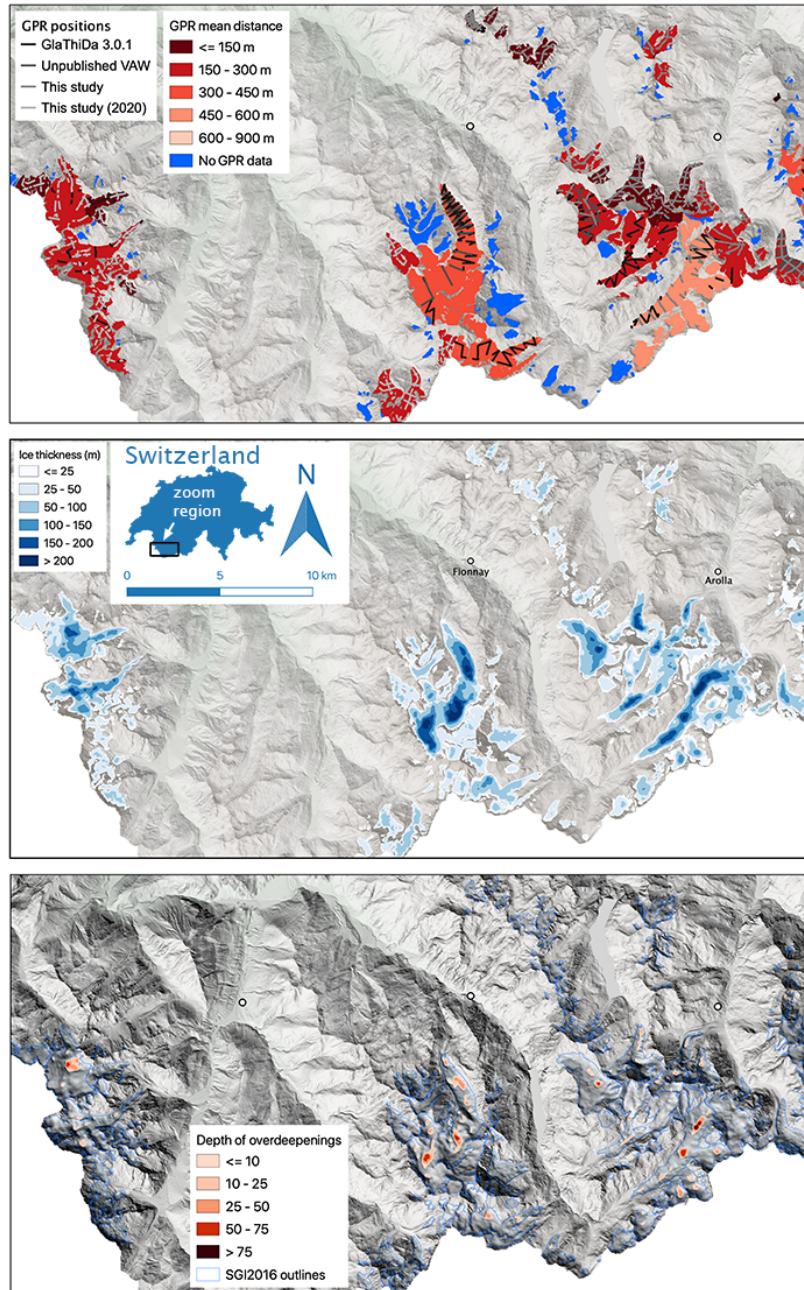


Figure S2: Region A, south-western Valais: (a) in blue are the glaciers for which no GPR data has been measured to date. In red are glaciers for which GPR data exists, with the color-code indicating the density of the data coverage expressed by the mean of the distances of all points on the glacier to the closest GPR-measurement point. Gray lines indicate location of the GPR-measurement points. (b) Interpolated ice thickness distribution. (c) Hillshade of the glacier-bed topography within SGI2016 outlines and color-coded the depth of overdeepenings. Background: Hillshade from the swissALTI3D after Swisstopo (2019)

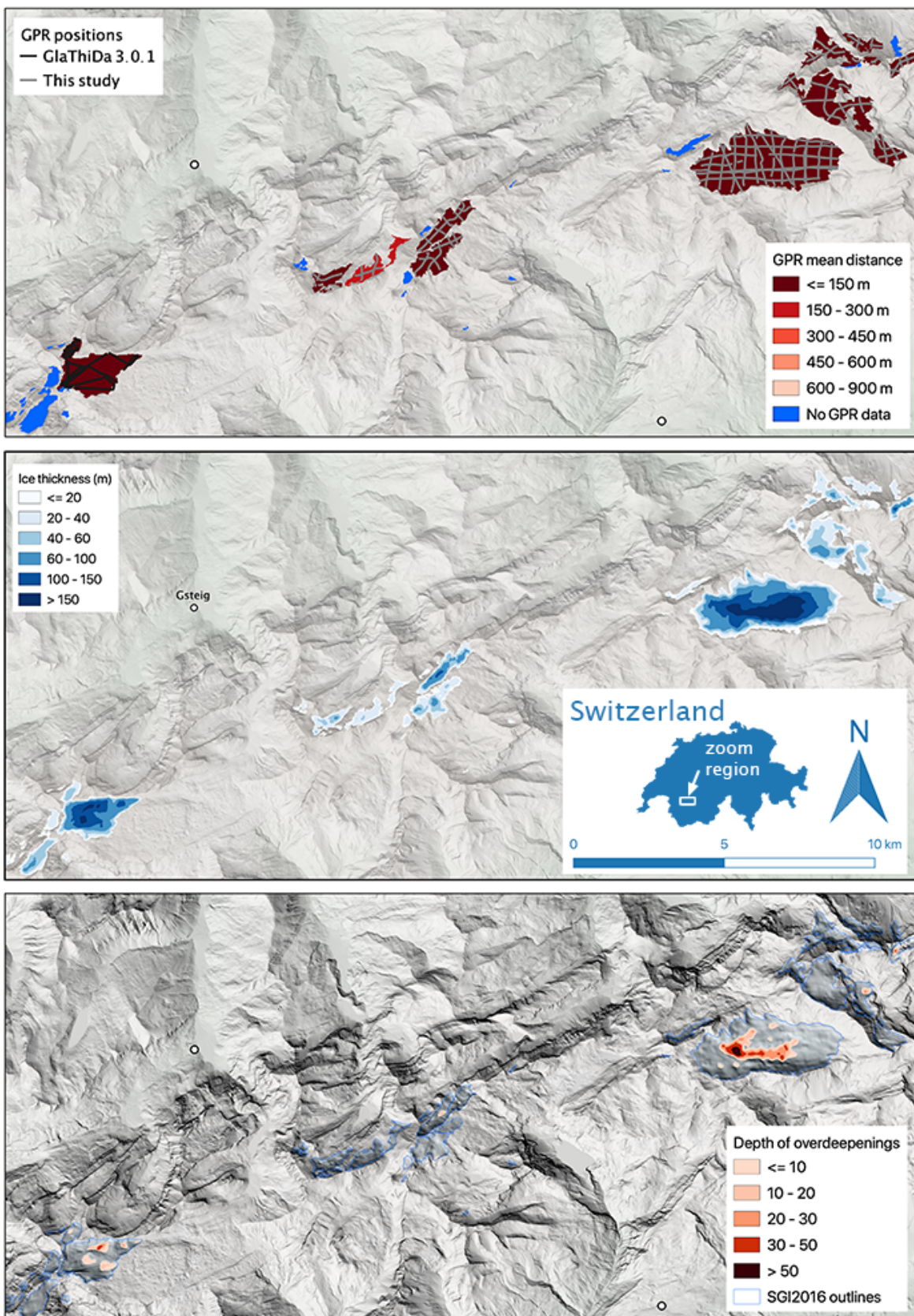


Figure S3: Region B, north-western Valais: (a) in blue are the glaciers for which no GPR data has been measured to date. In red are glaciers for which GPR data exists, with the color-code indicating the density of the data coverage expressed by the mean of the distances of all points on the glacier to the closest GPR-measurement point. Gray lines indicate location of the GPR-measurement points. (b) Interpolated ice thickness distribution. (c) Hillshade of the glacier-bed topography within SGI2016 outlines and color-coded the depth of overdeepenings. Background: Hillshade from the swissALTI3D after Swisstopo (2019)

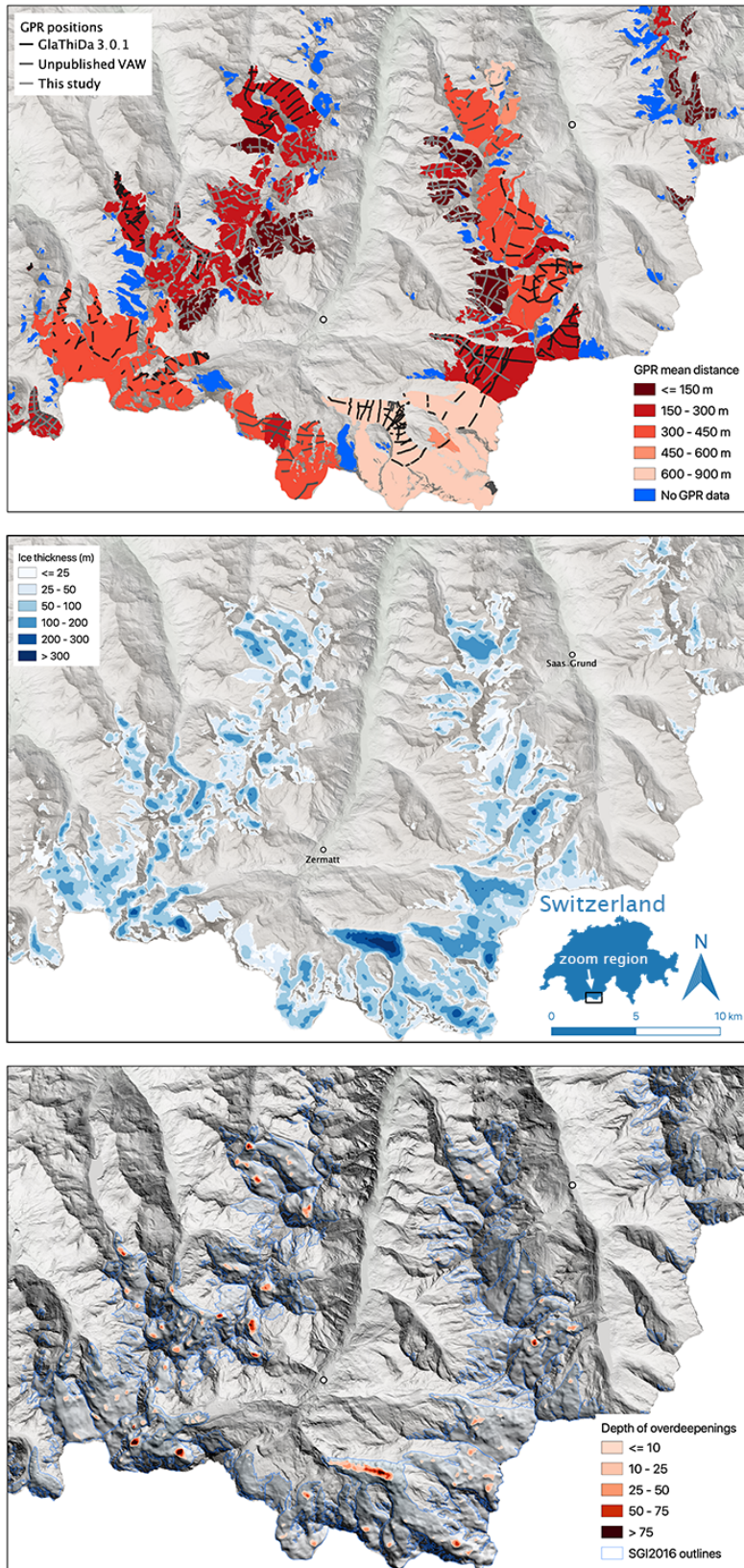


Figure S4: Region C, south-eastern Valais: (a) in blue are the glaciers for which no GPR data has been measured to date. In red are glaciers for which GPR data exists, with the color-code indicating the density of the data coverage expressed by the mean of the distances of all points on the glacier to the closest GPR-measurement point. Gray lines indicate location of the GPR-measurement points. (b) Interpolated ice thickness distribution. (c) Hillshade of the glacier-bed topography within SGI2016 outlines and color-coded the depth of overdeepenings. Background: Hillshade from the swissALTI3D after Swisstopo (2019)

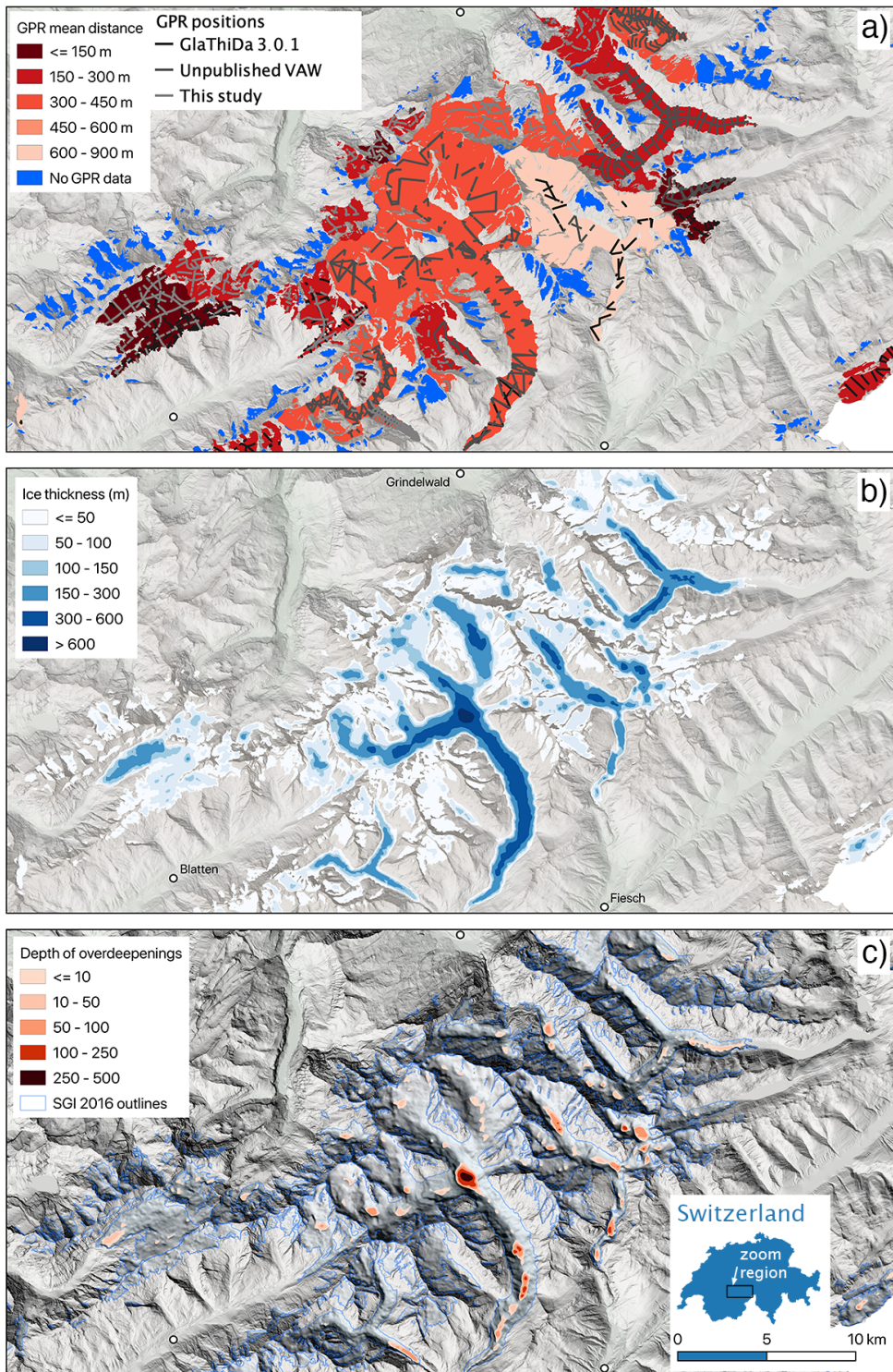


Figure S5: Region D, Bernese Alps: (a) in blue are the glaciers for which no GPR data has been measured to date. In red are glaciers for which GPR data exists, with the color-code indicating the density of the data coverage expressed by the mean of the distances of all points on the glacier to the closest GPR-measurement point. Gray lines indicate location of the GPR-measurement points. (b) Interpolated ice thickness distribution. (c) Hillshade of the glacier-bed topography within SGI2016 outlines and color-coded the depth of overdeepenings. Background: Hillshade from the swissALTI3D after Swisstopo (2019)

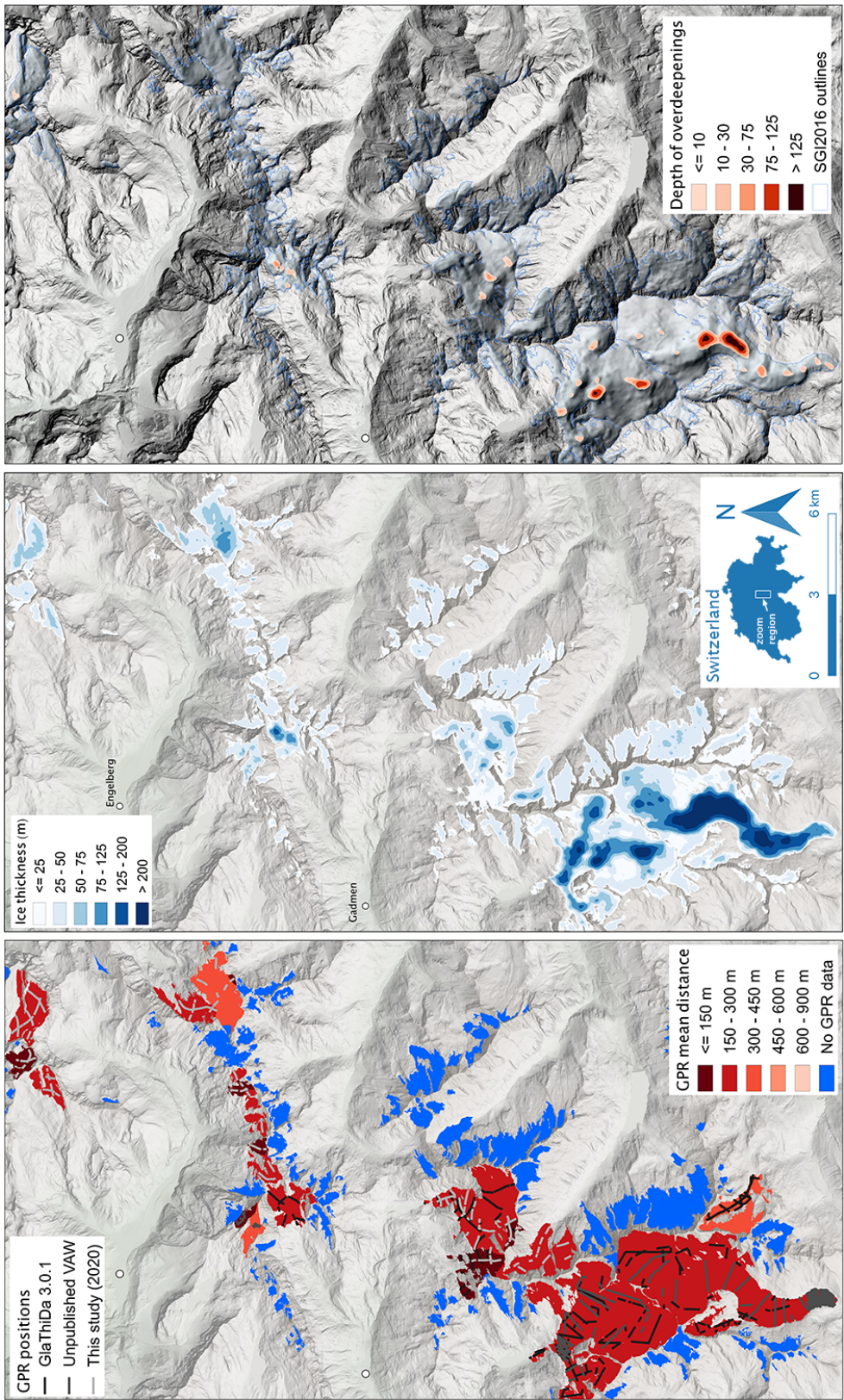


Figure S6: Region E, Uri Alps (rotated): (a) in blue are the glaciers for which no GPR data has been measured to date. In red are glaciers for which GPR data exists, with the color-code indicating the density of the data coverage expressed by the mean of the distances of all points on the glacier to the closest GPR-measurement point. Gray lines indicate location of the GPR-measurement points. (b) Interpolated ice thickness distribution. (c) Hillshade of the glacier-bed topography within SGI2016 outlines and color-coded the depth of overdeepenings. Background: Hillshade from the swissALTI3D after Swisstopo (2019)

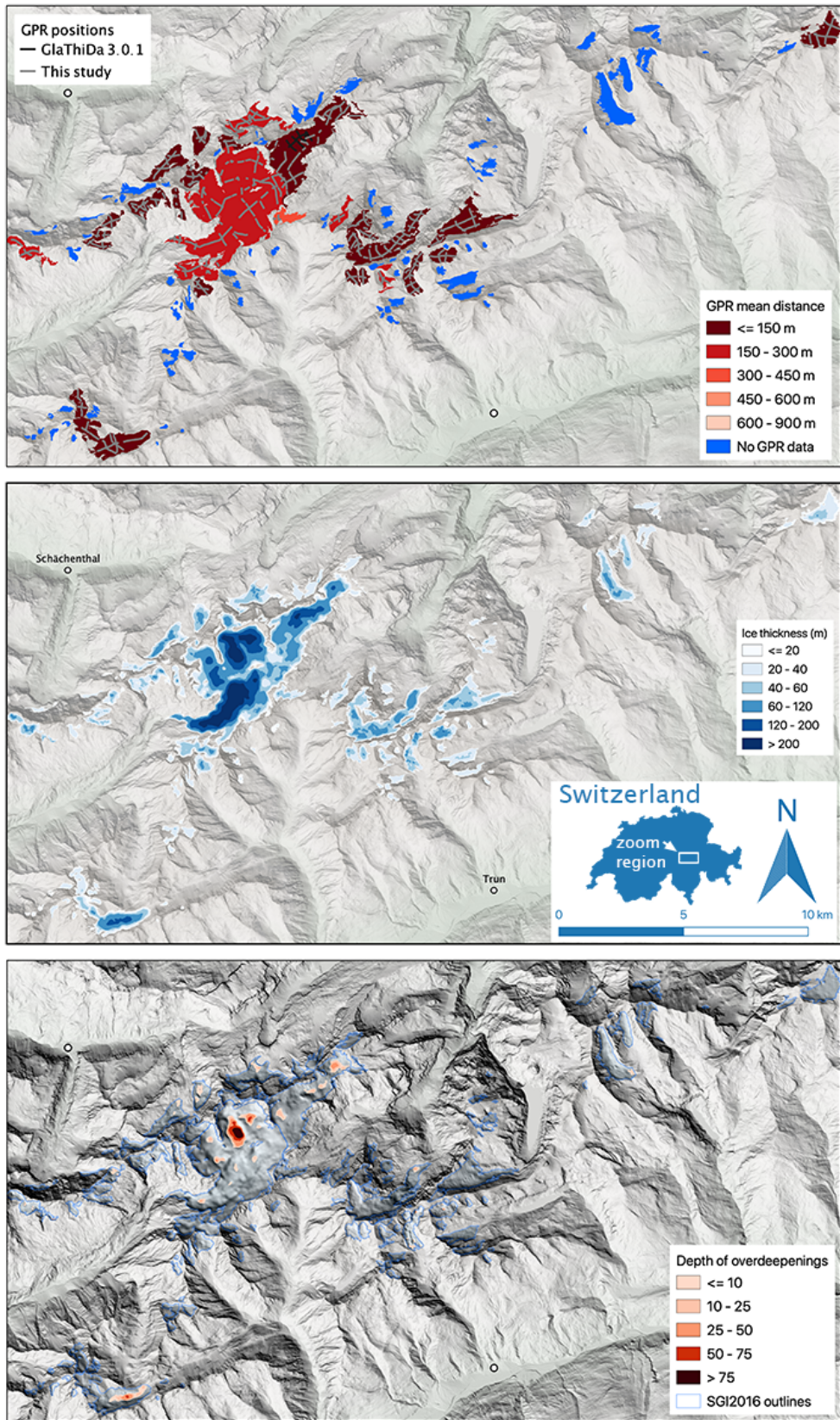


Figure S7: Region F, Glarus Alps: (a) in blue are the glaciers for which no GPR data has been measured to date. In red are glaciers for which GPR data exists, with the color-code indicating the density of the data coverage expressed by the mean of the distances of all points on the glacier to the closest GPR-measurement point. Gray lines indicate location of the GPR-measurement points. (b) Interpolated ice thickness distribution. (c) Hillshade of the glacier-bed topography within SGI2016 outlines and color-coded the depth of overdeepenings. Background: Hillshade from the swissALTI3D after Swisstopo (2019)

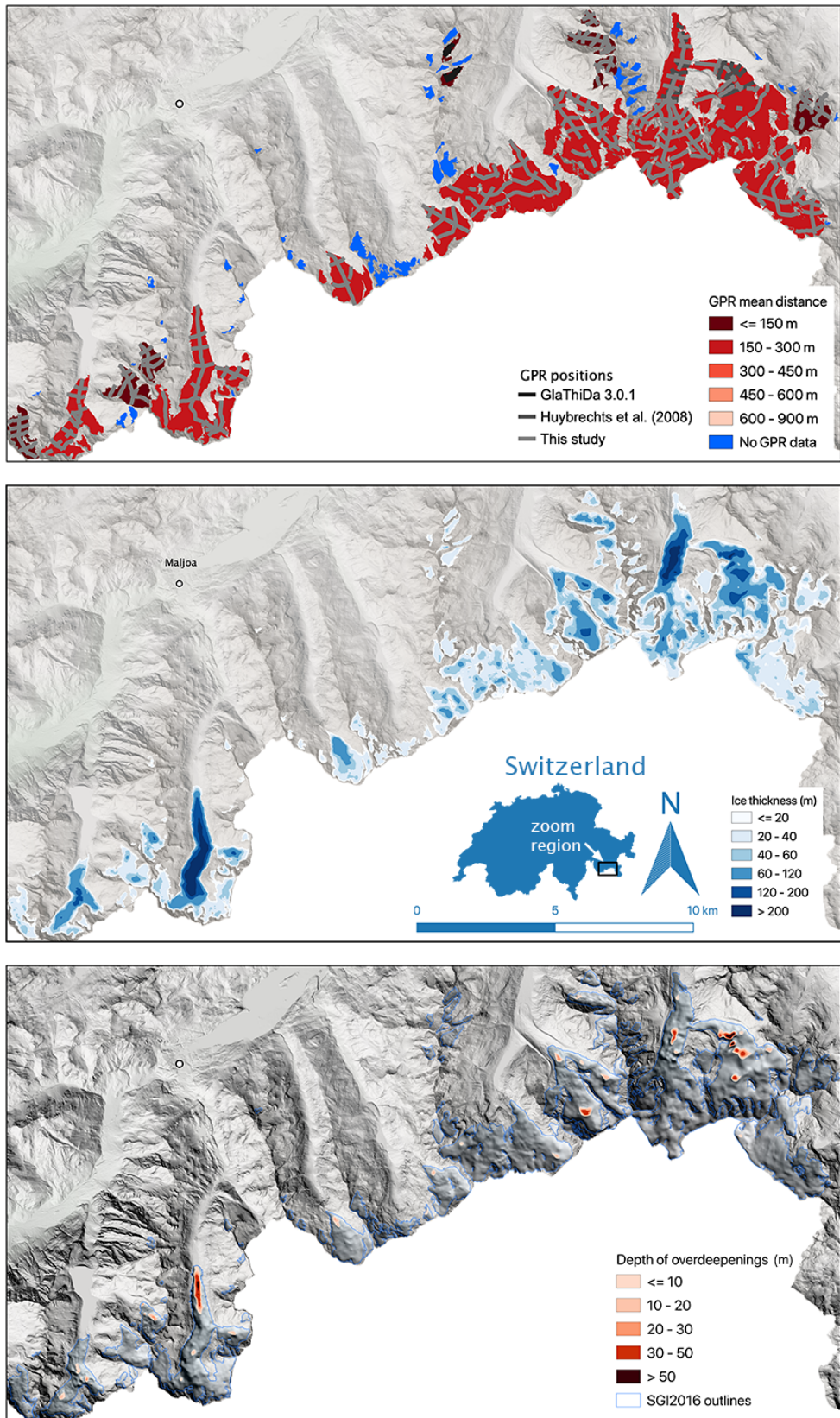


Figure S8: Region G, southern Grisons: (a) in blue are the glaciers for which no GPR data has been measured to date. In red are glaciers for which GPR data exists, with the color-code indicating the density of the data coverage expressed by the mean of the distances of all points on the glacier to the closest GPR-measurement point. Gray lines indicate location of the GPR-measurement points. (b) Interpolated ice thickness distribution. (c) Hillshade of the glacier-bed topography within SGI2016 outlines and color-coded the depth of overdeepenings. Background: Hillshade from the swissALTI3D after Swisstopo (2019)

### 3 Ice thickness distribution and overdeependings

From the data contained in SwissGlacierThickness-R2020, the total ice volume for individual river catchments can be calculated. This is shown in Fig. S9a, where the volumes homogenized for the year 2016 are displayed. We differentiated the catchments of the main river systems Rhône, Rhine, Po, and Inn, which all have their sources in the Swiss Alps. For catchments definitions see Fig. S10. Furthermore, the ice thickness distribution across specific elevation bands was calculated. The result is shown in Fig. S9b. It becomes evident that the maximum ice volume (asterisk symbol in Fig. S9) occurs at substantially different elevations for the different regions and therefore it is expected that the hydrology of each region responds differently to changes in climate. It is important to note here that the ice thickness distributions are given for the inventory years defined by the DEM (swissALTI3D, r2019) and thus exhibit some heterogeneity. These years are provided in SwissGlacierThickness-R2020 in the form of raster data and are displayed in Fig. S11. More details about the temporal meta data were presented by Weidmann et al. (2018).

We also analyzed the glacier bed topography provided in SwissGlacierThickness-R2020 with regard to the volumes of overdeepening. The locations of anticipated overdeepenings are displayed in Fig. S3-S8 with the color code indicating their depth. The volumes of these overdeepenings provide an estimate of future lake volumes. In Fig. S9c, the largest lake volumes are displayed separately for the corresponding glaciers. For the smaller lake volumes the volumes summed over several glaciers are shown. We note that more than half of this lake volumes occur in the glacier beds of only four glaciers.

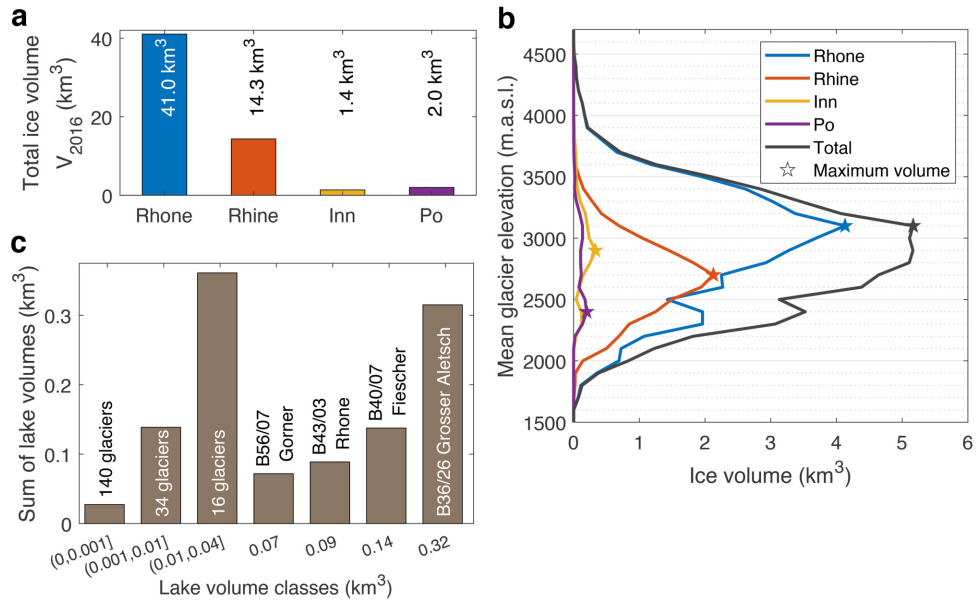


Figure S9: (a) Total ice volumes of glaciers located within the watersheds of the rivers Rhône, Rhine, Inn and Po. (b) Hypsometric ice volume distribution of the four river catchments and entire Swiss Alps, with elevation values referring to the mean of glacier bed and surface. Asterisk symbols indicate elevations where maximum volumes occur. (c) Sum of potential glacier lake volumes by lake volume classes (per glacier) with the four glaciers with largest lakes shown individually.

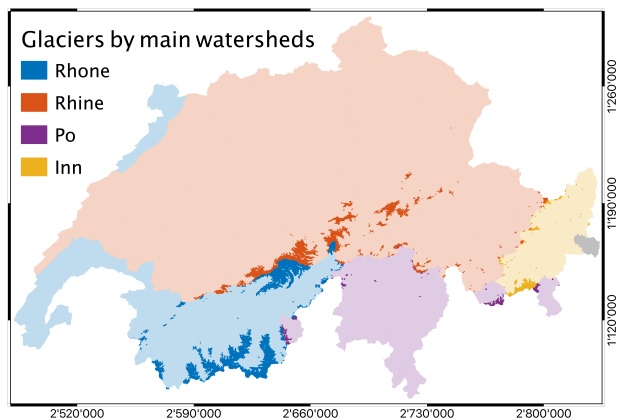


Figure S10: Dark colors: Outlines of Swiss glaciers color-coded by main watersheds. Light colors: watersheds within Swiss borders. In gray is the Adige watershed, which contains no glaciers within the Swiss borders.

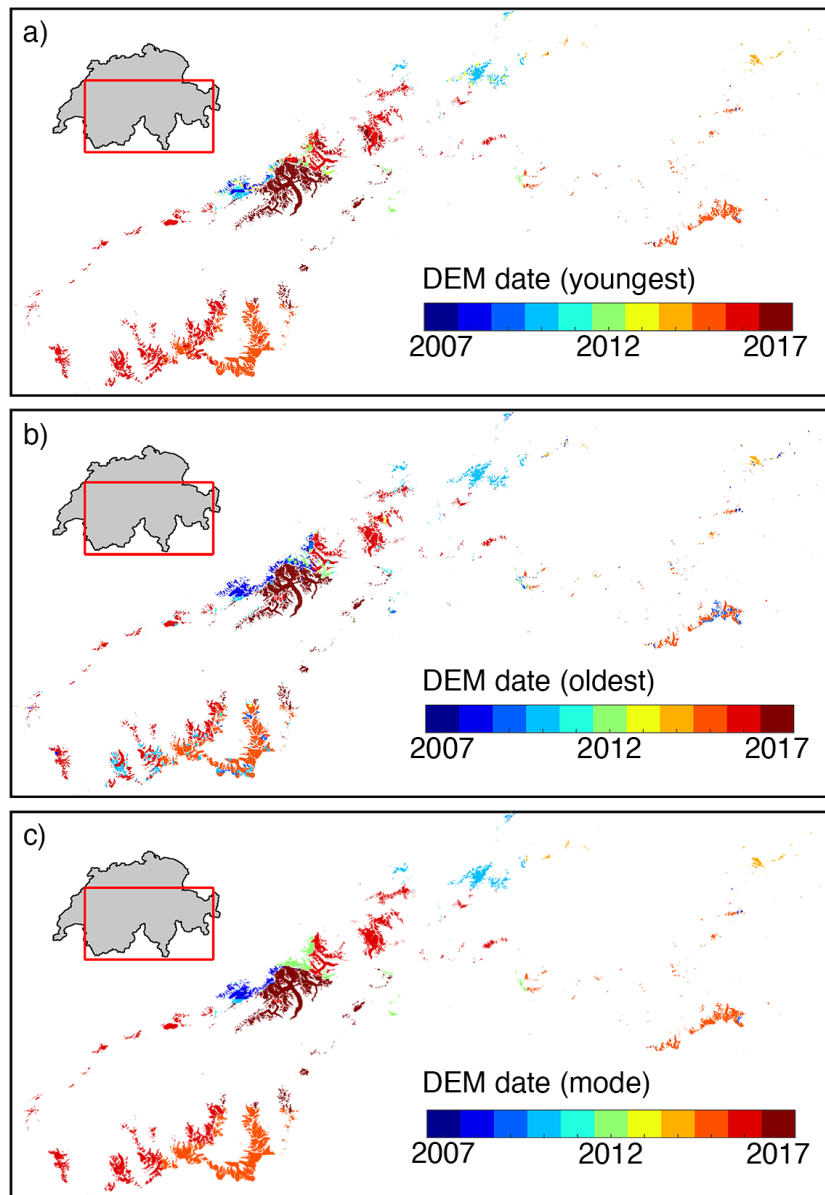


Figure S11: Recording years of the 2019-release of swissALTI3D (Swisstopo, 2019), reproduced from its metadata. (a) youngest year, (b) oldest year, (c) most frequently occurring (mode) year.

## 4 Supplementary Figures of the Uncertainty Analysis

In our publication, we present in Appendix C the calculation of point-specific ice thickness uncertainties  $u^\pm(x, y)$ . One of the components considered for computing  $u^\pm(x, y)$  is the uncertainties of the ice thickness interpolation  $u_{\text{int}}^\pm(x, y)$ . For illustrating the calculation of  $u_{\text{int}}^\pm(x, y)$ , explained in detail in the main manuscript, a supplementary illustration is provided here in Fig. S12.

Apart from the calculation of the uncertainty of the total ice volume in the Swiss Alps  $\bar{u}_V$ , explained in detail in Appendix D of our publication, we also computed the glacier-specific uncertainties of the ice volumes. Resulting values of these glacier-specific uncertainties are presented here in Fig. S13 for absolute uncertainties and in Fig. S14 for uncertainties normalized by each glacier's mean ice thickness.

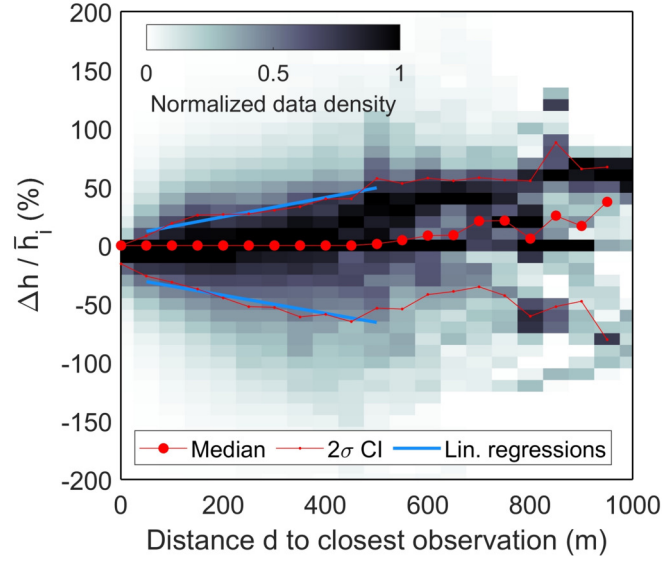


Figure S12: Deviations  $\Delta h$  of modelled and measured ice thickness normalized with the glacier-specific mean ice thickness  $\bar{h}_i$  versus distance  $d$  to the closest ice thickness observation. Gray-scale image: number of points falling within the corresponding area of the plot, normalized by maximum values within each discrete distance interval of 50 m width. Red symbols: median and  $2\sigma$ -confidence intervals for each distance interval. Blue lines: linear regression over distances up to 500 m, within which this data set is densely populated. See also Appendix C of the main manuscript.

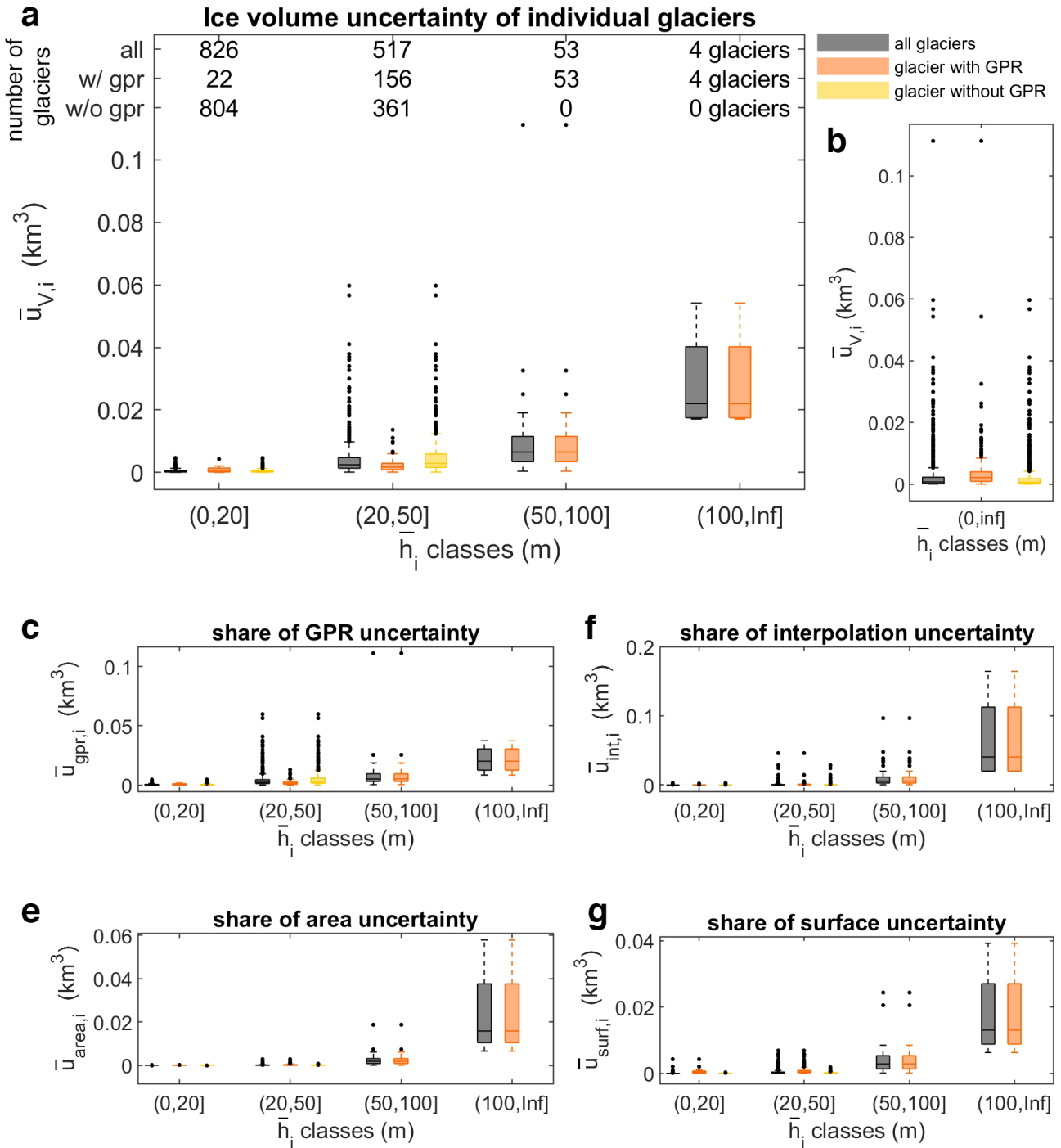


Figure S13: a) Distribution of ice volume uncertainties of individual glaciers,  $\bar{u}_{V,i}$ , for specific classes of mean ice thicknesses  $\bar{h}_i$  and separated for glaciers for which GPR data exists (red), for which no GPR data exists (yellow) and for glaciers with/without GPR data combined (black). For the calculation of  $\bar{u}_{V,i}$  see equation 4 of the main manuscript. Number of glaciers falling into certain mean ice thickness classes are listed. b) same as in (a) but not separated by classes of mean ice thicknesses. c)-f), same as in a) but for the individual components considered for computing  $\bar{u}_{V,i}$ , i.e. the input quantities of equation 4. Boxplots represent median, 25<sup>th</sup> and 75<sup>th</sup> percentiles, range without outliers and outliers.

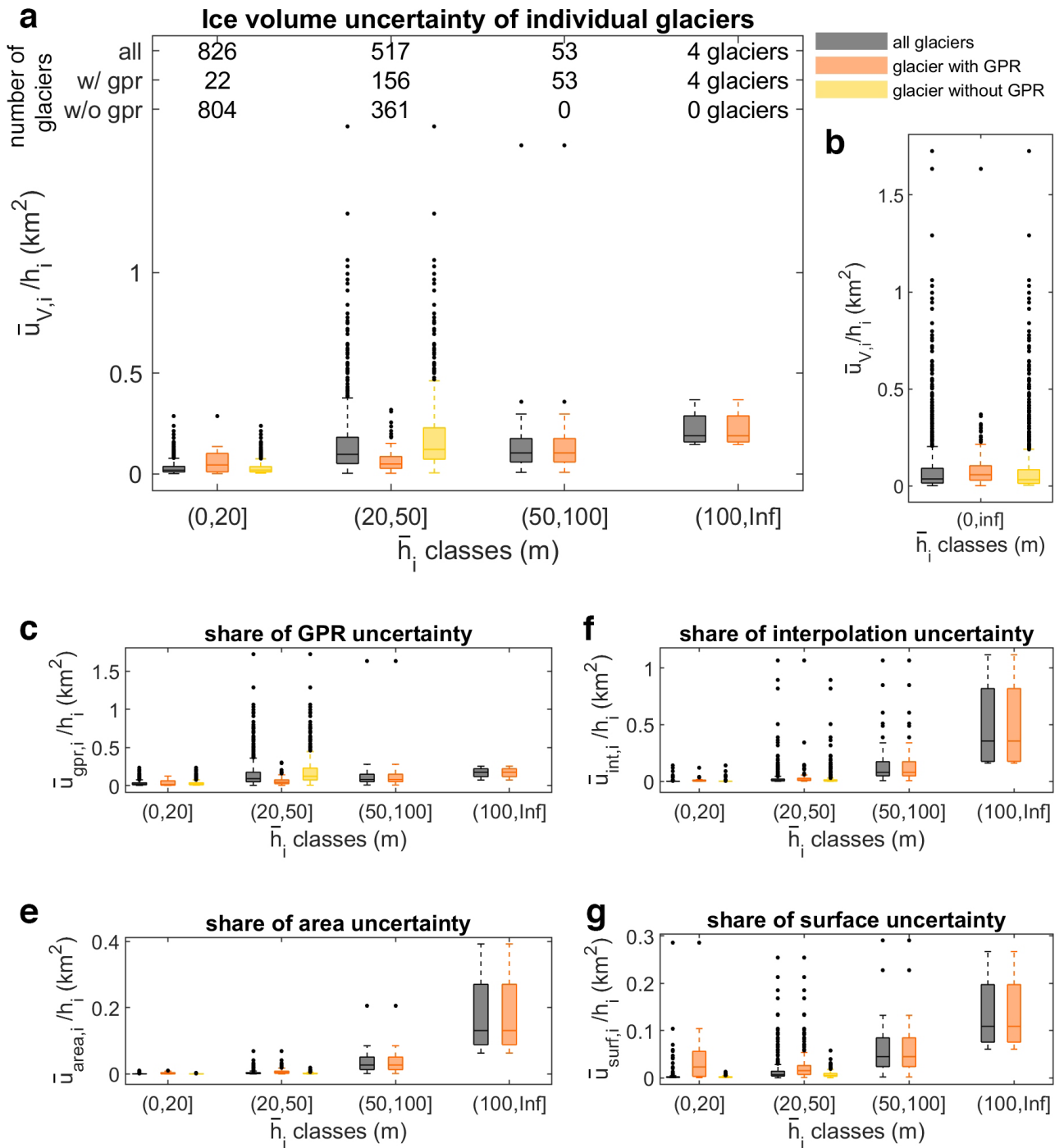


Figure S14: Same as Fig. S13 but with uncertainties normalized by each glacier's mean ice thickness.

## References

- Bauder, A., Funk, M., and Gudmundsson, G. H. (2003). The ice-thickness distribution of Unteraargletscher, Switzerland. *Annals of Glaciology*, 37:331–336.
- Capt, M., Bosson, J.-B., Fischer, M., Micheletti, N., and Lambiel, C. (2016). Decadal evolution of a very small heavily debris-covered glacier in an Alpine permafrost environment. *Journal of Glaciology*, 62(233):535–551.
- Farinotti, D., Huss, M., Bauder, A., and Funk, M. (2009). An estimate of the glacier ice volume in the Swiss Alps. *Global and Planetary Change*, 68(3):225–231.
- Feiger, N., Huss, M., Leinss, S., Sold, L., and Farinotti, D. (2018). The bedrock topography of Gries-and Findelen-gletscher. *Geographica Helvetica*, 73(1):1–9.
- Fischer, M., Haeberli, W., Huss, M., Paul, F., Linsbauer, A., and Hoelzle, M. (2013). Estimation of basal shear stresses from now ice-free LIA glacier forefields in the Swiss Alps. *EGUGA*, pages EGU2013–150.
- Funk, M., Gudmundsson, G. H., and Hermann, F. (1994). Geometry of the glacier bed of the Unteraargletscher, Bernese Alps, Switzerland. *Zeitschrift fuer Gletscherkunde und Glazialgeologie*, 30:187–194.
- GLAMOS (2020a). Swiss Glacier Ice Thickness, release 2020. Glacier Monitoring Switzerland, doi.org/10.18750/icethickness.2020.r2020.
- GLAMOS (2020b). Swiss Glacier Inventory 2016. Glacier Monitoring Switzerland, doi:10.18750/inventory.sgi2016.r2020.
- GlaThiDa Consortium, W. (2019). Glacier Thickness Database 3.0.1. *World Glacier Monitoring Service*. Zurich, Switzerland.
- Grab, M., Mattea, E., Bauder, A., Huss, M., Rabenstein, L., Hodel, E., Linsbauer, A., Langhammer, L., Schmid, L., Church, G., Hellmann, S., Délèze, K., Schaer, P., Lathion, P., Farinotti, D., and Maurer, H. (2020). SwissGlacierThickness-R2020. *ETH Research Collection*, DOI: 10.3929/ethz-b-000434697.
- Gudmundsson, G. H. (1994). Converging glacier flow - A case study: the Unteraarglacier, VAW Internal Report 131. *Mitteilungen der Versuchsanstalt fur Wasserbau, Hydrologie und Glaziologie an der Eidgenossischen Technischen Hochschule Zurich*.
- Huss, M. (2010). Mass balance of Pizolgletscher. *Geographica Helvetica*, 65(2):80–91.
- Huss, M., Farinotti, D., Bauder, A., and Funk, M. (2008). Modelling runoff from highly glacierized alpine drainage basins in a changing climate. *Hydrological processes*, 22(19):3888–3902.
- Huss, M. and Fischer, M. (2016). Sensitivity of very small glaciers in the Swiss Alps to future climate change. *Frontiers in Earth Science*, 4:34.
- Huybrechts, O., Rybak, O., Nemec, J., and Eisen, O. (2008). Towards a coupled three-dimensional glacier/mass balance model of the Morteratschgletscher, Engadin. In *EGU General Assembly 2008, Vienna, Austria 18 April 2008*.
- Lüthi, M. P. (1994). *Stabilität steiler Gletscher. Eine Studie ueber den Einfluss möglicher Klimaaenderungen. Untersuchungen am Beispiel eines Haengegletschers in der Westflanke des Eigers*. PhD thesis, Eidgenössische Technische Hochschule Zürich.
- Lüthi, M. P. (2000). Rheology of cold firn and dynamics of a polythermal ice stream (studies on Colle Gnifetti and Jakobshavns Isbrae). *Mitteilungen der Versuchsanstalt fur Wasserbau, Hydrologie und Glaziologie an der Eidgenossischen Technischen Hochschule Zurich*.
- Moll, A. (2012). *Tiefengletscher, Uri: Vergangenheits-und Gegenwartsanalyse, Eisradarmessungen zum Stand 2011 sowie Modellierungen einer zukünftigen möglichen Gletscherentwicklung*. PhD thesis, Geographisches Institut der Universität Zürich.
- Roethlisberger, H. and Funk, M. (1987). Schlussbericht ueber die Sondierungen 1986, Bericht No 20.4. *Mitteilungen der Versuchsanstalt fur Wasserbau, Hydrologie und Glaziologie an der Eidgenossischen Technischen Hochschule Zurich*.
- Rutishauser, A., Maurer, H., and Bauder, A. (2016). Helicopter-borne ground-penetrating radar investigations on temperate alpine glaciers: A comparison of different systems and their abilities for bedrock mapping. *Geophysics*, 81(1):WA119–WA129.

- Sharp, M., Richards, K., Willis, I., Arnold, N., Nienow, P., Lawson, W., and Tison, J.-L. (1993). Geometry, bed topography and drainage system structure of the Haut Glacier d'Arolla, Switzerland. *Earth Surface Processes and Landforms*, 18(6):557–571.
- Sugiyama, S., Bauder, A., Huss, M., Riesen, P., and Funk, M. (2008). Triggering and drainage mechanisms of the 2004 glacier-dammed lake outburst in Gornergletscher, Switzerland. *Journal of Geophysical Research: Earth Surface*, 113(F4).
- Swisstopo (2019). Bundesamt für Landestopografie swisstopo-swissALTI3D, Ausgabebericht 2019.
- Thyssen, F. and Ahmad, M. (1969). Ergebnisse seismischer Messungen auf dem Aletschgletscher. *Polarforschung*, 39(1):283–293.
- VAW (1998). Mauvoisin - Gietroglatscher - Corbassieregletscher. Glaziologische Studie im Zusammenhang mit den Stauanlagen Mauvoisin, im Auftrag der Elektrizitaetsgesellschaft. Report 55.05.7903, (M. Funk, unpublished, VAW ETH Zurich).
- VAW (2010). Adduction de Zinal, Expertise mandatee par les Forces Motrices de la Gougra SA. VAW ETH Zurich.
- VAW (2011). Gletscher- und Abflussentwicklung im Gebiet des Fieschergletschers 1900 - 2100. im Auftrag der Gommerkraftwerke AG, A. Bauder and D. Farinotti, unpublished, VAW ETH Zurich).
- VAW (2012). Eisdickenverteilung der Gletscher im Aletschgebiet. Radarmessungen an den Gletschern Grosser Aletsch, Oberaletsch, Mittelaletsch. im Auftrag der Electra-Massa AG, Kanton Wallis, Dienststelle Wald und Landschaft, Sion, Kanton Wallis, Dienststelle Energie und Wasserkraft, Sion (A. Bauder and N. Zoller, unpublished, VAW ETH Zurich ).
- VAW (2014a). Eisvolumen der Gletscher im Mattmarkgebiet. Radarmessungen und Bestimmung des Eisvolumens sowie dessen zeitliche Entwicklung seit 1931, im Auftrag der Kraftwerke Mattmark AG. Report No 7902.52.60 (A. Bauder and I. Frei, unpublished, VAW ETH Zurich).
- VAW (2014b). Radarmessungen auf dem Theodul- und Furggletscher, im Auftrag der Grande Dixence SA. unpublished, VAW ETH Zurich.
- VAW (2017a). Eisdickenmessungen auf dem Vadret dal Cambrena: Helikoptergestuetzte Radarmessungen. (A. Bauder and M. Grab, unpublished, VAW and IfG, ETH Zurich).
- VAW (2017b). Eisdickenverteilung und Gletscherbett-Topographie des Oberaletschgletschers: Helikoptergestuetzte Radarmessungen. (A. Bauder and M. Grab, unpublished, VAW ETH Zurich).
- VAW (2019). Ground-Penetrating Radar (GPR) investigations in the terminus area of Oberaletschgletscher. (D. Farinotti, H.R. Maurer, P. Carlen, M. Grab, and G. Church, unpublished, VAW and IfG, ETH Zurich).
- Waechter, H. and Roethlisberger, H. (1982). Internal report No 55.22. *Mitteilungen der Versuchsanstalt fur Wasserbau, Hydrologie und Glaziologie an der Eidgenossischen Technischen Hochschule Zurich*.
- Weidmann, Y., Gandor, F., and Artuso, R. (2018). Temporale Metadaten swissALTI3D. *Geomatik Schweiz*, page 11.